

SPECTRAL AND MORPHOMETRIC PROPERTIES OF THE FRACASTORIUS CRATER LUNAR DOME. C. Ahrens¹ and R. Lena², ¹ORAU/Solar System Exploration Division, NASA GSFC, Greenbelt, MD 20771 (Caitlin.ahrens@nasa.gov); ²Lunar Domes Coordinator, Assoc. of Lunar and Planetary Observers, Rome, Italy.

Introduction: The Fracastorius dome (-18.94°N, 33.02°E) is situated at the northern rim of Fracastorius crater (-21.36°N, 33.07°E), a 120.6-km diameter crater cutting into the south of the Mare Nectaris basin (Figure 1). The dome is elongated, with a putative vent on its surface, with some asymmetry of its flanks. The average flank slope is ~1° near the vent, but the eastern flank is steepest (~2.7°). The dome has a diameter of 28.6 km and height of 241.5 m.

In this study, we use the morphologic and morphometric characteristics of the dome as a basis for estimation of its yield strength, viscosity, eruption rate, eruption duration, and make assumptions on the feeder dike geometry (e.g., dike length and width). We then compare these values to other known effusive lunar domes from [1] and [2].

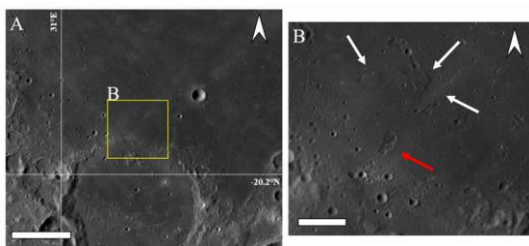


Figure 1: A) LROC image of southern Mare Nectaris and Fracastorius crater. Scale bar 50 km. B) Subset image of the Fracastorius dome. Scale bar 10 km. White arrows indicate the northern flanks of the dome. Red arrow marks the irregular vent structure.

Methods: Lunar image data from the Lunar Reconnaissance Orbiter (LRO) Wide-angle camera (WAC; 100 m/px) and Narrow-angle camera (NAC; ~32 m/px) were used to map the parameters of the Fracastorius dome. The Lunar Orbiter Laser Altimeter (LOLA) data was then used (using 64 ppd maps) to create digital elevation models (DEMs) to determine the diameter and height of the dome, along with the vent morphology.

Clementine UVVIS spectral data has been calibrated and normalized, as provided by [3]. The TiO₂ content derived by the abundance maps were created from topographically correct mineral reflectance maps acquired by the JAXA Selene/Kaguya. Chandrayann-1's Moon Mineralogy Mapper (M³) data were calibrated and photometrically

corrected and converted to apparent reflectance. The spectral continuum is the line connecting the reflectance values at 750 nm and 1500 nm, by which the reflectance spectrum is divided to obtain the continuum-removed spectrum [4].

Results:

Spectral results: The R_{415}/R_{750} color ratio is a measure for the TiO₂ content of basaltic soils, where high ratios correspond to high TiO₂ content and vice versa [5]. The R_{950}/R_{750} color ratio is related to the strength of the mafic absorption band and is sensitive to the optical maturity of mare and highland materials [6]. The Fracastorius dome is revealed to have a reflectance of $R_{750} = 0.1273$, a low value for the UVVIS color ratio of $R_{415}/R_{750} = 0.6010$ and a $R_{950}/R_{750} = 1.0647$, indicating low TiO₂ content. This TiO₂ content is measured to be ~2 wt.%, while the FeO content varies 12 – 14 wt.%.

The M³ spectrum of Fracastorius dome displays a trough ~1000 nm with a minimum wavelength at 980 nm and an absorption band ~2200 nm (Figure 2). This corresponds to a typical high-Ca pyroxene signature [7], indicating a basaltic composition.

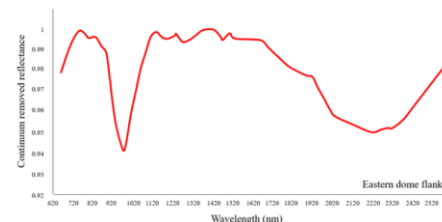


Figure 2: Mineralogical characteristics of the Fracastorius eastern dome flank from M3 spectrum.

Effusion rate and duration: We presume that magma erupting from a dome-forming structure would spread outward onto a flat plane in all directions, as proposed by [2]. Such a model regarding the properties of the dome and magma behavior would estimate the yield strength τ , i.e. the pressure that must be exceeded for the lava to flow, the fluidity of the erupted lava with plastic viscosity η , and the effusion rate E (i.e., lava volume erupted per second) [1]. From this rheological model by [2], the flow is treated as a Bingham plastic (expressed in Pa), which we use a value of 2000 kg/m³ as used in several previous studies

[1, 2], $g = 1.63 \text{ m s}^{-2}$, h the height of the dome, and D the dome diameter, where h and D are measured from the elevation profiles. Plastic viscosity η [Pa s] is:

$$\eta = 6 \times 10^{-4} \tau^{2.4}$$

We obtained values for $\tau = 4.28 \times 10^3 \text{ Pa}$ and $\eta = 3.12 \times 10^5 \text{ Pa s}$. From h and D , we estimate the volume of the dome to be $V = 77.4 \text{ km}^3$.

The rheologic model developed by [2] depends on D , h , V , and ρ , and the effective flow thickness ($c_f \cdot h$). However, it should be noted that this assumption is not straightforward to determine as it is unknown if the ad hoc assumption of measuring c_f halfway between the dome summit and rim appropriately reflects the effective flow thickness [8].

The relation for the effusion rate is then

$$E = \frac{0.323^{0.5} 300 \kappa \left(\frac{D}{2}\right)^2}{0.65^{\frac{5}{2}} c_f^2 h}$$

where $\kappa = 10^{-6} \text{ m}^2 \text{ s}^{-1}$ as the thermal diffusivity of the lava [2, 9]. We calculated E to be $5.91 \times 10^2 \text{ m}^3 \text{ s}^{-1}$. Using V and E , we calculated that the duration of the lava effusion, probably from multiple eruption events at the Fracastorius dome, is $T \sim 4.15$ years.

Dike geometry: These inferred rheological properties can be used to model the geometry of the subsurface dike through which the magma ascended, and the magma rise speed U , given dike length L and width W , as described in more detail in our report [10]. Using the rheological properties τ and η determined earlier, together with the eruption rate of $5.91 \times 10^2 \text{ m}^3 \text{ s}^{-1}$, we find that the dike width $W = 11.8 \text{ m}$. We can then determine the magma rise speed by balancing the driving pressure gradient against the wall friction and allowing for overcoming the yield strength by [2]. The magma rise speed is calculated to be $2.1 \times 10^{-4} \text{ m/s}$.

Assuming a mean crustal density $\rho_c = 2800 \text{ kg/m}^3$ and the magma density of $\rho = 2000 \text{ kg/m}^3$, the effusion rate E are related to the dike geometry L and W and magma ascension speed U , thus making dike length $L = 234 \text{ km}$.

Table 1 shows the results using magma densities of $\rho = 1600, 2000, 2400$, and 3000 kg/m^3 (from [2]) to give a possible range of dike geometries at Fracastorius dome.

Table 1: Values of the magma rise speed (U), dike width (W), and dike length (L) at Fracastorius dome as a function of varying magma densities.

Morphometric Parameter	1600 kg/m ³	2000 kg/m ³	2400 kg/m ³	3000 kg/m ³
Magma rise speed (U) [m/s]	2.9×10^{-4}	2.1×10^{-4}	1.1×10^{-4}	3.8×10^{-5}
Dike width (W) [m]	10.02	11.8	16.8	27.86
Dike length (L) [km]	200	234	330	559

Conclusions: In this study we have examined the lunar dome in Mare Nectaris and Fracastorius crater in terms of the spectral and morphometric properties and the eruption conditions. The dome has also been observed to have a basaltic composition using Clementine and Chandrayaan-1 M³ spectral data. The Fracastorius dome formed from lavas with viscosities around 3.12 Pa s , with an effusion rate $\sim 5.91 \times 10^2 \text{ m}^3 \text{ s}^{-1}$ over a time period of ~ 4.2 years, probably from multiple effusive eruption events. With this slope degree and comparatively large volume, the Fracastorius dome probably consisted of a lower lava temperature and thus an increased degree of crystallization during magma ascent. The rheological properties inferred that the feeder dike has a geometry of 11.8 m width and 234 km length.

Acknowledgments: Ahrens is supported by an appointment to the NASA Postdoctoral Program at the NASA Goddard Space Flight Center administered by Oak Ridge Associated Universities (ORAU) under contract with NASA.

References: [1] Lena, R., Wöhler, C., Bregante, M. T., Lazzarotti, P., & Lammel, S. (2008). PSS, 56(3-4), 553-569. [2] Wilson, L., & Head, J. W. (2003). JGR: Planets, 108(E2). [3] Eliason, E., Isbell, C., Lee, E., Becker, T., Gaddis, L., McEwen, A., & Robinson, M. (1999). LPI, Houston. PDS volumes USA NASA PDS CL 4001 4078. [4] Lena, R., Wöhler, C., Phillips, J., & Chiocchetta, M. T. (2013). Lunar Domes (pp. 39-48). Springer, Milano. [5] Charette, M. P., McCord, T. B., Pieters, C., & Adams, J. B. (1974). JGR, 79(11), 1605-1613. [6] Lucey, P. G., Blewett, D. T., & Hawke, B. R. (1998). JGR: Planets, 103(E2), 3679-3699. [7] Besse, S., Sunshine, J. M., & Gaddis, L. R. (2014). JGR: Planets, 119(2), 355-372. [8] Lena, R., Wöhler, C., Phillips, J., Wirths, M., & Bregante, M. T. (2007). PSS, 55(10), 1201-1217. [9] Lena, R., Wöhler, C., Phillips, J., Sellini, M., Zompatori, D., & Group, G. L. R. G. (2009). PSS, 57(3), 267-275. [10] Ahrens, C., & Lena, R. (2022). Remote Sensing, 14(23), 6135.